NANO LETTERS

pubs.acs.org/NanoLett Letter

Conformal Prelithiation Nanoshell on $LiCoO_2$ Enabling High-Energy Lithium-Ion Batteries

Xiaoxiao Liu, Yuchen Tan, Wenyu Wang, Chunhao Li, Zhi Wei Seh, Li Wang, and Yongming Sun*

Cite This: *Nano Lett.* 2020, 20, 4558−4565 Read Online

ACCESS | Metrics & More | Article Recommendations | Supporting Information

ABSTRACT: The initial lithium loss in lithium-ion batteries (LIBs) reduces their energy density (e.g., 15% or higher for LIBs using a Si-based anode). Herein, we report *in situ* chemical formation of a conformal Li_2O/Co nanoshell (~20 nm) on $LiCoO_2$ particles as a high-capacity built-in prelithiation reagent to compensate this initial lithium loss. We show a 15 mAh g^{-1} increase in overall charge capacity for the $LiCoO_2$ with 1.5 wt % Li_2O/Co in comparison to the pristine $LiCoO_2$ in virtue of the irreversible lithium extraction from the nanoshell ($4Li_2O + 3Co \rightarrow 8Li^+ + 8e^- + Co_3O_4$, $2Li_2O \rightarrow 4Li^+ + 4e^- + O_2\uparrow$). Paired with a graphite−SiO anode, a full cell using such a $LiCoO_2$ cathode demonstrates 11% higher discharge capacity (2.60 mAh cm^{-2}) than that using pristine $LiCoO_2$ (2.34 mAh cm^{-2}) at 0.1 *C*, as well as stable battery cycling. Moreover, the prelithiated $LiCoO_2$ is compatible with the current battery fabrication process.

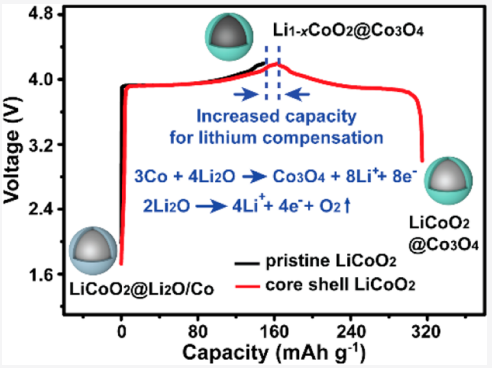

KEYWORDS: *lithium-ion batteries, cathode prelithiation, $LiCoO_2$, high energy*

Lithium-ion batteries (LIBs) using $LiCoO_2$ as the cathode and graphite as the anode are the dominant power sources for portable electronics.[1−3] Since their commercialization by Sony in 1991, the energy density of $LiCoO_2$||graphite batteries has been increasing from 75 to over 200 Wh kg^{-1} accompanied by the improvement of electrode materials and electrolytes, which is approaching the limit with regard to the theoretical capacity of graphite (372 mAh g^{-1}), practical reversible capacity of $LiCoO_2$ (~140 mAh g^{-1}), and electrochemical window of current electrolytes (<4.3 V). The further increase in energy density of the $LiCoO_2$-based LIBs relies on the development of stabilized $LiCoO_2$ that can release higher reversible capacity (e.g., >160 mAh g^{-1}) in a wider working potential window (e.g., 3−4.5 V),[4−6] electrolytes with larger electrochemical window (e.g., 0−4.5 V),[7−9] and Si-based anode with higher capacity (e.g., >450 mAh g^{-1}) in comparison to those in traditional commercial LIBs.[10,11] The Si-based anode ranks among the most promising alternatives for the current commercial pure graphite anode for next-generation high-energy density LIBs due to its higher capacity and similar working potential.[12] However, the Si-based anode suffers from much lower initial Coulombic efficiency than graphite, typically ~85% for the graphite−Si or graphite−SiO composite with a capacity of ~450 mAh g^{-1}, which further decreases with increased Si content. In other words, an appreciable amount of active lithium from the cathode is consumed accompanied by the formation of a solid electrolyte interphase (SEI) on the anode surface during the initial battery charging process. This initial lithium loss significantly reduces the overall capacity and energy density of LIBs.

The $LiCoO_2$ cathode is the only lithium source in LIBs with a lithium-free graphite or Si-based anode. Loading additional $LiCoO_2$ at the cathode side can compensate this initial lithium loss. However, this approach would increase the mass loading at the cathode side and the improvement in energy density is very limited due to the low practical lithium-ion capacity of $LiCoO_2$ (~140 mAh g^{-1}). Electrochemical prelithiation approaches (e.g., discharging a Si nanowire||Li metal cell) showed high lithium compensation efficiency, but the complex operation limits their practical application.[13,14] Prelithiation additives are promising to compensate the initial lithium loss. Stabilized lithium metal powders (SLMPs), lithium silicide, and Li_xZ−Li_2O composites (Z = Si, Ge, Sn, etc.) can be effective lithium donors to offset the initial lithium loss when used as anode prelithiation additives and introduced into the anode due to their high lithium-ion capacities.[15−18] However, their high chemical reactivity makes them challenging for practical application, which causes safety concerns and is not compatible with the regular industrial slurry-based electrode fabrication using *N*-methyl-pyrrolidone (NMP) or water as the solvent. Although cathode prelithiation additives, such as Li_2NiO_2, Li_6CoO_4, and Li_5FeO_4, show better stability than

Received: April 1, 2020
Revised: April 25, 2020
Published: May 6, 2020

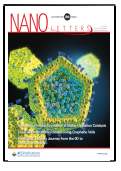

https://dx.doi.org/10.1021/acs.nanolett.0c01413
Nano Lett. 2020, 20, 4558−4565

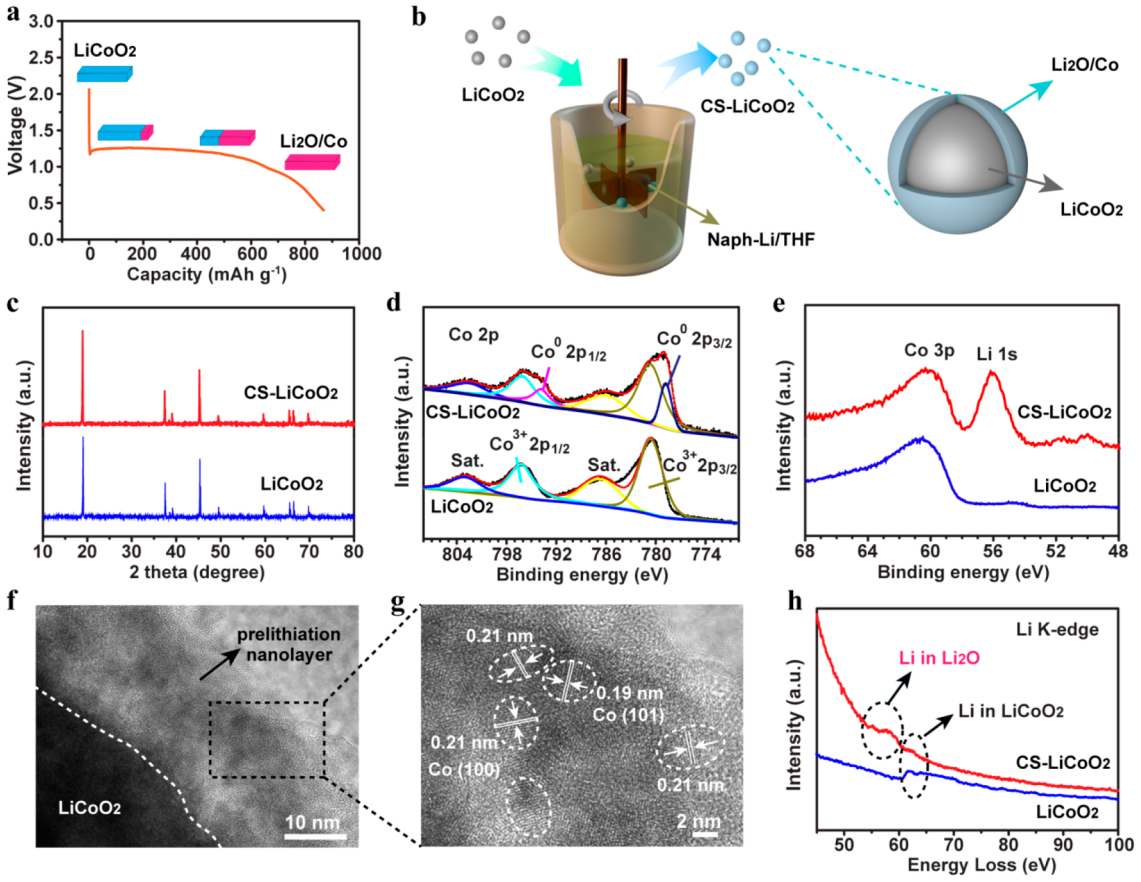

Figure 1. (a) Capacity−voltage plot of $LiCoO_2$ during its electrochemical lithiation process at 0.1 *C*. The inset illustrates the intermediate products during the conversion reaction of $LiCoO_2$. (b) Schematic illustration of the preparation of CS-$LiCoO_2$. (c) XRD patterns and (d, e) high-resolution Co 2p, Co 3p, and Li 1s XPS spectra of the pristine $LiCoO_2$ and CS-$LiCoO_2$. (f) TEM image of a CS-$LiCoO_2$ particle and (g) high-resolution TEM image on the edge of the CS-$LiCoO_2$ particle in Figure f. (h) EELS spectra of the pristine $LiCoO_2$ and CS-$LiCoO_2$.

anode prelithiation additives, their "donor" lithium-ion capacity is limited (e.g., <400 mAh g^{-1}).[19−21] Li_2O, Li_2O_2, and Li_3N can release high "donor" lithium-ion capacity, but their application as prelithiation additives is not compatible with the current battery or electrode manufacturing process.[22−24] Recently, we successfully fabricated a series of cathode prelithiation additives (Li_2O/M, M = Fe, Co, Ni, etc.) through the reaction between metal oxide and molten lithium, which released high "donor" lithium-ion capacities (e.g., >600 mAh g^{-1}) based on the inverse conversion reaction (Li_2O/M → M + xLi^+ + xe^-) in the initial battery charge process and improved the reversible capacity and energy density of the full cells up to 11%.[25−27] However, facile materials synthesis with high safety should be explored before their scale-up application.

Prelithiation materials for LIBs should follow the guidelines below in consideration of the practical application: (1) High "donor" lithium-ion capacity during the initial charging process without causing negative effects on cycle life or rate capability of the LIBs. (2) Controllable prelithiation degree, which is critical for the capacity matching between the cathode and anode to maximize the overall energy density of LIBs. (3) Good compatibility with the current battery fabrication processes, including slurry fabrication, electrode drying, and battery assembly. (4) Simple and straightforward materials processing with low cost and high safety.

Herein, we propose the rational design of a functional cathode that consists of active material with a high-capacity built-in prelithiation reagent in each single particle. The built-in prelithiation reagent can provide a high "donor" lithium-ion capacity during the first cycle to compensate the initial lithium loss, and the active material can release reversible capacity for battery cycling. Experimentally, a simple and low cost solution chemistry route utilizing the reaction between $LiCoO_2$ and a lithium complex (lithium naphthaline, Naph-Li, $Li^+C_{10}H_8^-$) solution was used to *in situ* generate a conformal ultrathin Li_2O/Co nanoshell on $LiCoO_2$ particles. It is noteworthy that the reaction between $LiCoO_2$ and lithium complex is controllable. The thickness of the Li_2O/Co nanoshell can be tuned to meet different requirements of lithium compensation for batteries using different anodes. Importantly, the materials, electrode, and battery processing can be carried out using current industrial technology for the as-achieved CS-$LiCoO_2$. In comparison to using independent prelithiation materials, our implanted prelithiation reagent in cathode materials simplifies the electrode fabrication process and enables more uniform prelithiation in comparison to using individual prelithiation reagents. Therefore, our strategy for the compensation of the initial lithium loss and increase of energy density of LIBs meets the as-mentioned criteria for scalable application. As an example, we showed that the CS-$LiCoO_2$ with appropriate prelithiation (1.5 wt % Li_2O/Co in the CS-$LiCoO_2$) exhibited a 15 mAh g^{-1} higher charge specific capacity than the pristine $LiCoO_2$ (165 mAh g^{-1} for the CS-$LiCoO_2$ vs 150 mAh g^{-1} for the pristine $LiCoO_2$) at 0.1 *C*. A CS-$LiCoO_2$||graphite−SiO full cell exhibited higher capacity

https://dx.doi.org/10.1021/acs.nanolett.0c01413
Nano Lett. 2020, 20, 4558−4565

and energy density than the counterpart using pristine $LiCoO_2$ as well (533 Wh kg^{-1} for CS-$LiCoO_2$||graphite−SiO cell vs 481 Wh kg^{-1} for $LiCoO_2$||graphite−SiO cell).

RESULTS AND DISCUSSION

$LiCoO_2$ is a well-known conventional layered cathode in the typical $R\bar{3}m$ space group with the *a*-$NaFeO_2$ crystal structure (Figure S1). Lithium ions are occupied between the octahedral metal oxide slabs within the structure and can be reversibly extracted/inserted through the topotactic reaction.[28] When additional lithium ions are electrochemically introduced into $LiCoO_2$, continuous electrochemical conversion takes place to form a Li_2O/Co nanocomposite ($LiCoO_2 + 3Li^+ + 3e^- \rightarrow 2Li_2O + Co$, Figure 1a).[29,30] This reaction starts from the surface of $LiCoO_2$ particles and gradually penetrates the entire particle. Before the full lithiation, $LiCoO_2$ and Li_2O/Co coexist as the intermediates, with a tiny amount of Li_2O/CoO at their interface.[31] These results make it possible to fabricate a Li_2O/Co or Li_2O/CoO/Co nanocomposite on each single $LiCoO_2$ particle as a built-in high-capacity prelithiation material via an electrochemical and/or chemical route. While the reaction for the fabrication of Li_2O/Co nanocomposite on $LiCoO_2$ particles is precisely controllable using an electrochemical process by assembling an electrochemical cell, it is time-consuming and the operation is complex and not suitable for the practical industrial application. Here, a simple and controllable solution based reaction was explored to *in situ* form a Li_2O/Co nanocomposite shell on $LiCoO_2$ utilizing the chemical reaction between lithium complex (Li^+B^-) and $LiCoO_2$ at room temperature (Figure 1b). Li^+B^- is composed of a positively charged lithium ion (Li^+) and a negatively charged organic ligand (B^-).[32] Lithium naphthaline (Naph-Li, $Li^+C_{10}H_8^-$) complex was chosen in virtue of its low cost and easy preparation. During the synthesis, 0.2 M Naph-Li solution in tetrahydrofuran (THF) was prepared through the reaction between metallic Li and naphthalene in THF at room temperature. The $LiCoO_2$ powder was then immersed into the as-fabricated Naph-Li solution. Electrons transferred from $C_{10}H_8^-$ to the surface of $LiCoO_2$ particles and Li^+ ions incorporated into $LiCoO_2$ simultaneously during the reaction, leaving uncharged state naphthalene in the THF solution. Residual naphthalene in the $LiCoO_2$ cathode could be easily removed during the washing and baking process due to its high solubility in THF and low sublimation temperature (Figure S2). By controlling the ratio of Naph-Li and $LiCoO_2$ (molar ratio of 3.7/100), 1.2 wt % of the $LiCoO_2$ was chemically lithiated, corresponding to 1.5 wt % of Li_2O/Co in the CS-$LiCoO_2$. The reaction solution turned from the initial dark blue to light yellow after 3 min, indicating the fast reaction between Naph-Li and $LiCoO_2$ (Figure S3). Finally, a Li_2O/Co nanoshell was *in situ* formed uniformly on the very surface of $LiCoO_2$ particles. Note that the remaining naphthalene in the THF solution can be reused to fabricate the Naph-Li solution, making the fabrication of CS-$LiCoO_2$ recyclable and low-cost. Only active lithium was introduced into the $LiCoO_2$ cathode through such a facile processing, and thus, high prelithiation efficiency for the as-achieved prelithiation material (Li_2O/Co) could be expected. We can tune the content of the Li_2O/Co composite in the CS-$LiCoO_2$ through regulating the initial amount of $LiCoO_2$ and Li-Naph (Figure S4). The simple solution-based chemical prelithiation route avoids the complicated operation process for electrochemical prelithiation and is more efficient in comparison to the synthesis and use of individual cathode prelithiation reagents, making it a promising strategy for addressing the initial lithium loss in LIBs.

The morphology and structure of the CS-$LiCoO_2$ were investigated using scanning electron microscopy (SEM), X-ray diffraction (XRD), and transmission electron microscopy (TEM). Figure S5a and b compared the SEM images of the pristine $LiCoO_2$ and CS-$LiCoO_2$. They both consisted of micrometer-sized irregular particles with similar morphology. No cracks or breaking were observed for the CS-$LiCoO_2$ particles, indicating the chemical prelithiation only took place on the very surface layer of $LiCoO_2$ particles but did not penetrate single $LiCoO_2$ particles and cause collapse due to the chemical conversion reaction with large volume expansion. In addition, there was no change in XRD peaks for CS-$LiCoO_2$ in comparison to the pristine $LiCoO_2$ (Figure 1c), suggesting that only a very small amount of $LiCoO_2$ converted to Li_2O/Co during the chemical conversion reaction. The composition and electronic structure of the surface layer of the CS-$LiCoO_2$ were investigated by X-ray photoelectron spectroscopy (XPS). High-resolution Co 2p, Co 3p, and Li 1s spectra for the pristine $LiCoO_2$ and CS-$LiCoO_2$ were compared in Figure 1d and e. In comparison with the pristine $LiCoO_2$, the peaks for Co 2p and Co 3p of CS-$LiCoO_2$ broadened and shifted to lower binding energy, demonstrating that the Co element on the surface of CS-$LiCoO_2$ was reduced during the chemical prelithiation process. Signals for Co metal (793.6 and 778.1 eV for Co^0 $2p_{1/2}$ and Co^0 $2p_{3/2}$, respectively) were observed in the Co 2p spectra (Figure 1d), indicating the formation of Co nanoparticles during the chemical prelithiation reaction.[25,29,33] Moreover, the CS-$LiCoO_2$ exhibited a much stronger peak for Li 1s in comparison to the pristine $LiCoO_2$, demonstrating the successful formation of a lithium-rich layer on $LiCoO_2$ particles during the chemical prelithiation reaction. A smooth surface was observed for a pristine $LiCoO_2$ particle under TEM, and its nature of the single crystal is revealed by the high-resolution TEM (HRTEM) image that shows the clear interplanar spacing of 0.24 nm corresponding to the (101) plane of $LiCoO_2$ (Figure S5). After chemical prelithiation, a thin layer of ∼20 nm was formed on the surface of $LiCoO_2$ particles (Figure 1f and Figure S5c). The HRTEM image of the Li_2O/Co composite was shown in Figure 1g. Abundant crystalline nanoparticles with a diameter of less than 5 nm were observed. These crystalline nanoparticles showed interplanar spacings of 0.19 and 0.21 nm corresponding to the (101) and (100) planes for metallic Co, respectively.[34] Electron energy loss spectroscopy (EELS) was further conducted for the surface layer of the CS-$LiCoO_2$ (Figure 1h). It is confirmed that the Li in $LiCoO_2$ was transformed to Li_2O after prelithiation.[25] As such, an ultrathin surface layer of the Li_2O/Co nanocomposite with a thickness of ∼20 nm was successfully formed on $LiCoO_2$ particles to produce CS-$LiCoO_2$ through the chemical reaction between $LiCoO_2$ and Naph-Li solution, which was consistent with the XPS results. This ultrathin Li_2O/Co nanolayer can be employed as a built-in prelithiation reagent of $LiCoO_2$ to provide high lithium-ion capacity and compensate the lithium loss at the anode and contribute to the improvement of the energy density of LIBs. Moreover, the result observed here regarding the structural change of $LiCoO_2$ during lithiation is also well consistent with the electrochemical prelithiation of $LiCoO_2$ or its chemical lithiation observed using *in situ* TEM measurement.[31]

The electrochemical performance of the pristine $LiCoO_2$ and CS-$LiCoO_2$ was investigated by galvanostatic charge−

https://dx.doi.org/10.1021/acs.nanolett.0c01413
Nano Lett. 2020, 20, 4558−4565

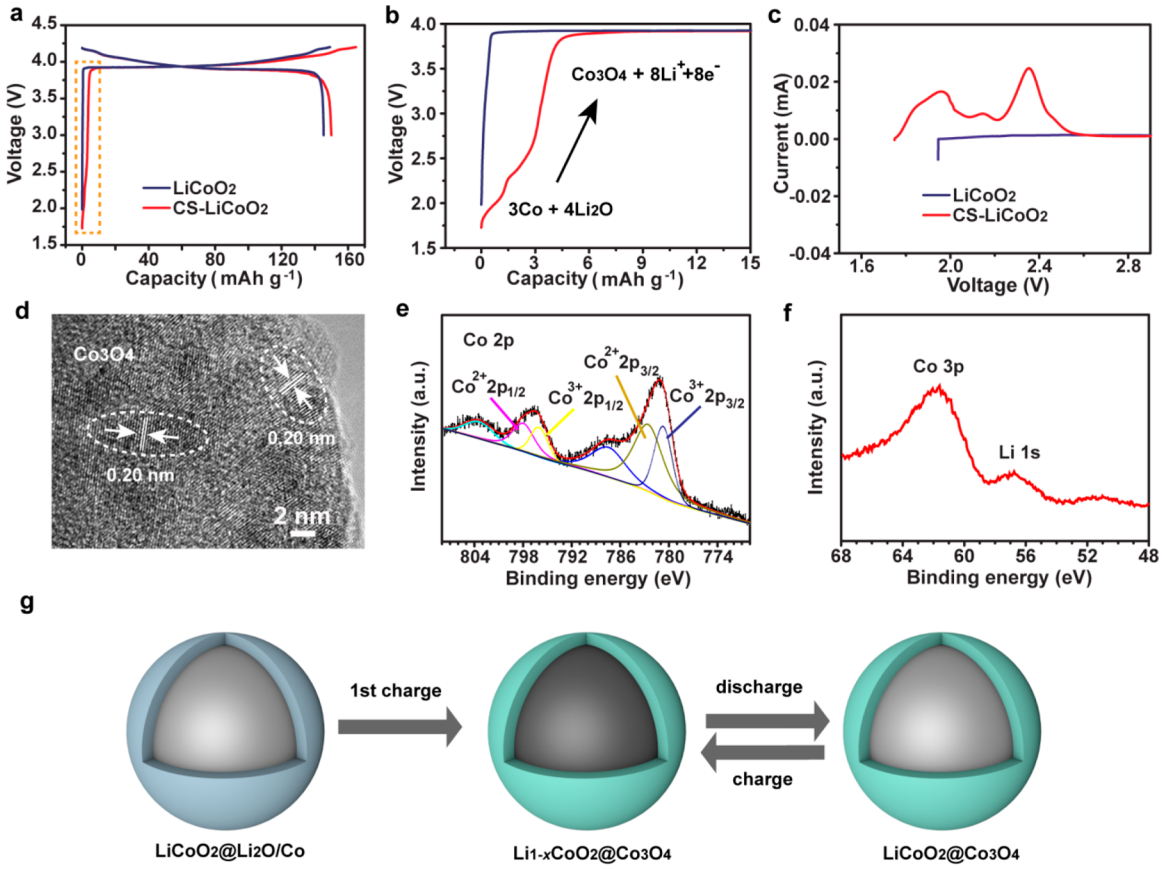

Figure 2. (a, b) The first-cycle charge/discharge curves of the pristine $LiCoO_2$ and CS-$LiCoO_2$ with the interior box enlarged. (c) Magnified CV profiles of the pristine $LiCoO_2$ and CS-$LiCoO_2$ electrodes in the potential range of 1.5−2.9 V. (d) HR-TEM image and high-resolution (e) Co 2p and (f) Co 3p and Li 1s XPS spectra of the CS-$LiCoO_2$ cathode after the first charge/discharge process. Co_3O_4 nanocrystals were observed at the surface of the CS-$LiCoO_2$, indicating the irreversible lithium extraction from the initial Li_2O/Co composite. (g) Schematic illustration of the structure evolution of the CS-$LiCoO_2$ cathode during the first charge and the following charge/discharge cycles.

discharge measurement in the potential range of 3−4.2 V in half cells using lithium metal as the counter electrode at 0.1 *C* (1 *C* = 140 mAh g^{-1}). Figure 2a and b showed the initial charge−discharge curves for the pristine $LiCoO_2$ and CS-$LiCoO_2$ electrodes. Overall, both electrodes exhibited similar voltage curves. It was noted that several small voltage plateaus were observed during the initial charge process below 3 V for the CS-$LiCoO_2$ electrode, which were different from the pristine $LiCoO_2$ electrode. Correspondingly, the differential capacity versus voltage (dQ/dV) profiles of the CS-$LiCoO_2$ electrodes (Figure S6) displayed obvious peaks in this voltage range. We further analyzed the cyclic voltammograms (CVs) for the pristine $LiCoO_2$ and CS-$LiCoO_2$ electrodes (Figure 2c). Several new oxidation peaks appeared between 1.7 and 2.7 V in the CVs of the CS-$LiCoO_2$ electrode in comparison to the pristine $LiCoO_2$ at a scan rate of 0.1 mV s^{-1}, well consistent with their charge−discharge profiles (Figure 2a and b). These new voltage plateaus or oxidation peaks for the CS-$LiCoO_2$ can be ascribed to the electrochemical lithium extraction from the Li_2O/Co nanocomposite, which can enable increased initial charge specific capacity for the CS-$LiCoO_2$ in comparison to the pristine $LiCoO_2$. The increased capacity during this voltage range was 8 mAh g^{-1}, which was close to the theoretical capacity contribution based on the inverse conversion reaction ($4Li_2O + 3Co \rightarrow 8Li^+ + 8e^- + Co_3O_4$). The slopes/plateaus between 3.7 and 4.2 V for both electrodes arose from the reversible extraction and insertion of lithium ions from/into the structure of $LiCoO_2$, contributing to the reversible capacity of $LiCoO_2$. Interestingly, the capacity during this voltage range for the CS-$LiCoO_2$ was ∼7 mAh g^{-1} higher than the pristine $LiCoO_2$ electrode. This increased capacity should be mainly contributed by the decomposition of residual Li_2O in the nanoshell ($2Li_2O \rightarrow 4Li^+ + 4e^- + O_2\uparrow$).[22] As expected, due to the capacity contribution from the prelithiation nanolayer of Li_2O/Co, the overall voltage−capacity curve of the CS-$LiCoO_2$ electrode shifted right and a high initial charge capacity of 165 mAh g^{-1} was delivered, which was 15 mAh g^{-1} higher than that for the pristine $LiCoO_2$ (150 mAh g^{-1}). The initial discharge curves of the pristine $LiCoO_2$ and CS-$LiCoO_2$ overlapped well and their discharge capacities were 145 and 150 mAh g^{-1}, respectively, suggesting no negative effect on the discharge process of $LiCoO_2$ for the chemical prelithiation treatment of $LiCoO_2$. The slightly increased discharge capacity of the CS-$LiCoO_2$ may come from the activation of $LiCoO_2$ during the materials processing. XRD was further conducted to investigate the structure information on the pristine $LiCoO_2$ and CS-$LiCoO_2$ at the discharge (to 3 V) and charge (to 4.2 V) states (Figure S7). The pristine $LiCoO_2$ and CS-$LiCoO_2$ exhibited a similar evolution for the locations and intensities of XRD peaks and no additional peaks were detected for the CS-$LiCoO_2$, suggesting that the chemical prelithiation did not cause the change in the reversible electrochemical lithium storage mechanism for $LiCoO_2$. Information for the structure and composition of the CS-$LiCoO_2$ after a full charge and

https://dx.doi.org/10.1021/acs.nanolett.0c01413
Nano Lett. 2020, 20, 4558−4565

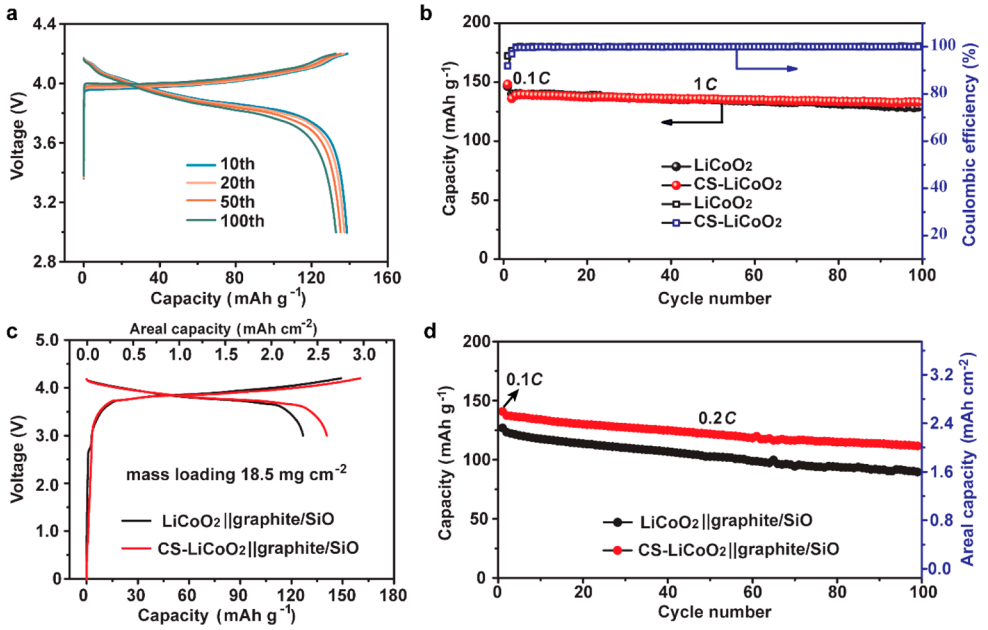

Figure 3. (a) Charge/discharge curves of CS-$LiCoO_2$ after the first cycle at 1 *C*. (b) Cycling comparison between the pristine $LiCoO_2$ and CS-$LiCoO_2$ electrodes in half cells. (c) The first-cycle charge/discharge curves and (d) cycling performance of the pristine $LiCoO_2$||graphite/SiO and CS-$LiCoO_2$||graphite/SiO full cells.

discharge cycle was also investigated using TEM and XPS. Observed under TEM, the thickness of the initial surficial layer on CS-$LiCoO_2$ was slightly reduced and maintained close contact with the $LiCoO_2$ core (Figure S8). Co_3O_4 nanocrystals with an average particle size of ~5 nm were observed on the surface of the CS-$LiCoO_2$ after one charge/discharge cycle (Figure 2d), demonstrating the oxidation of metallic Co and the irreversible extraction of lithium from the Li_2O/Co composite nanolayer in the working voltage range of $LiCoO_2$. The peak location of Co 2p in the high-resolution Co 2p XPS spectra shifted to higher binding energy (798.2 and 782.8 eV for Co^{2+} and 796.2 and 780.6 eV for Co^{3+}) after one charge/discharge cycle (Figure 2e), indicating the conversion of the initial Co state (metal Co) to a higher oxidation state (Co_3O_4).[33,35] The peak intensity of Li 1s was significantly reduced, which elucidated that lithium in the surficial layer of the CS-$LiCoO_2$ was irreversibly extracted during the charging process (Figure 2f). These results revealed that the Li_2O/Co nanocomposite transferred to Co_3O_4 and thus could deliver a high lithium-ion capacity during the charging process of the CS-$LiCoO_2$, and would not be lithiated in the discharging process. The conversion reaction of cobalt oxides takes place below 2 V, which is far below the cutoff voltage of $LiCoO_2$ (e.g., 3 V or even higher). As such, the as-produced Co_3O_4 would not be lithiated anymore after the first cycle during cycling. The "donor" lithium ions in the first-cycle charge process can compensate the initial lithium loss at the anode side, allowing the more electrochemically active lithium to be available and improving the energy density of LIBs. Since the extraction of lithium from Li_2O/Co only takes place during the first charge process, it will not have any negative effect on the following cycling. After donating lithium in the first charging process, the generated thin Co_3O_4 shell on the CS-$LiCoO_2$ cathode would remain unchanged during the following cycles. According to the above discussion, therefore, the Li_2O/Co nanoshell of CS-$LiCoO_2$ is promising as a built-in prelithiation material, which can compensate the lithium loss at the anode side and enable increased energy density for LIBs.

Figure 3a showed the charge/discharge curves of the CS-$LiCoO_2$ electrode in the lithium metal half cell after the first cycle at 1 *C*. The oxidation peaks below 3 V in the first-cycle charging process (Figure 2a) disappeared, and the $LiCoO_2$ and CS-$LiCoO_2$ electrodes showed similar voltage−capacity plots in the following cycles (Figure 3a and Figure S9), suggesting the electrochemical lithium extraction process from the Li_2O/Co nanocomposite only took place in the first cycle. Moreover, the pristine $LiCoO_2$ and CS-$LiCoO_2$ electrodes displayed similar electrochemical cycling stability (Figure 3b) and structure stability for 100 cycles (Figure S10), demonstrating that the chemical prelithiation here did not cause any negative effects on $LiCoO_2$. Besides, both electrodes maintained their initial structure (Figure S11) and showed similar EIS results on cycling (Figure S12), again verifying that the chemical prelithiation posed no threat to the cycling performance of the $LiCoO_2$ cathode.

With high "donor" lithium-ion capacity in the first cycle, the CS-$LiCoO_2$ electrode is promising for pairing with the high-capacity graphite−SiO anode to compensate the initial lithium loss and produce LIBs with high energy density. Since the Li_2O/Co nanocomposite is *in situ* formed on the surface of CS-$LiCoO_2$ and works as a built-in prelithiation reagent, no additional additive needs to be involved as an individual component during the slurry and electrode fabrication, which makes the processing industrially feasible. At a high mass loading of active material in cathodes (~18.5 mg cm^{-2}), the CS-$LiCoO_2$||graphite−SiO cell delivered higher discharge capacities than the $LiCoO_2$||graphite−SiO cell in the initial cycle at 0.1 *C* (141 mAh g^{-1} and 2.60 mAh cm^{-2} for CS-$LiCoO_2$||graphite−SiO vs 127 mAh g^{-1} and 2.34 mAh cm^{-2} for $LiCoO_2$||graphite−SiO, Figure 3c). Note that this specific capacity here was based on the total mass of $LiCoO_2$ or CS-$LiCoO_2$. This result indicated that the initial lithium loss at the graphite−SiO anode was successfully compensated by the

https://dx.doi.org/10.1021/acs.nanolett.0c01413
Nano Lett. 2020, 20, 4558−4565

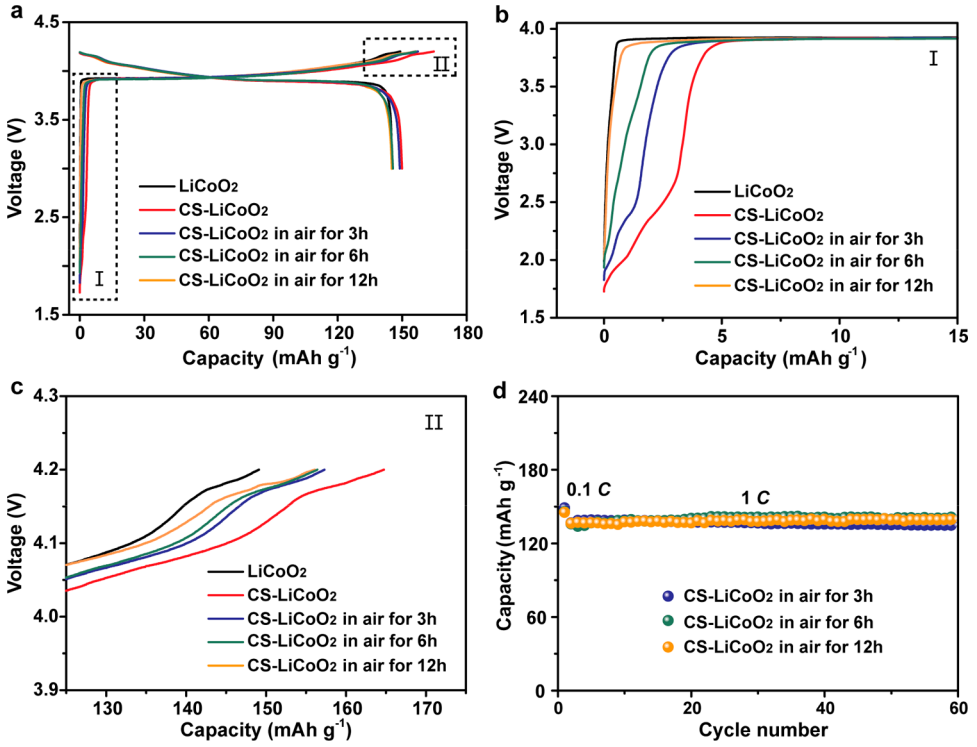

Figure 4. (a) First-cycle charge−discharge curves of the CS-$LiCoO_2$ electrodes exposed to ambient air conditions for different times (3, 6, and 12 h). (b, c) The enlarged boxes of I and II in Figure a. (d) Cycling performance of the CS-$LiCoO_2$ electrodes exposed to ambient air condition for different times (3, 6, and 12 h).

"donor" lithium ions from the Li_2O/Co composite and thus the overall energy density of batteries was significantly increased. The energy density of the CS-$LiCoO_2$||graphite−SiO cell was 533 Wh kg^{-1}, which was much higher than 481 Wh kg^{-1} for the pristine $LiCoO_2$||graphite−SiO cell, which was calculated based on the total mass of the cathode material. The charge−discharge curves and cycling stability were further compared for the CS-$LiCoO_2$||graphite−SiO and pristine $LiCoO_2$||graphite−SiO cells (Figure S13 and Figure 3d). After 100 cycles at a current density of 0.2 *C*, the CS-$LiCoO_2$||graphite−SiO cell still delivered a specific capacity of 112 mAh g^{-1} and an areal capacity of 2.09 mAh cm^{-2}, much higher than the values of 90 mAh g^{-1} and 1.65 mAh cm^{-2} for the pristine $LiCoO_2$||graphite−SiO cell.

The ambient stability of the as-fabricated material is important in consideration of its practical application in the battery industry. The electrochemical performance of CS-$LiCoO_2$ electrodes was evaluated after exposure to ambient air conditions for different times (3, 6, and 12 h). As shown in Figure 4a and b, the charge voltage plateaus of CS-$LiCoO_2$ electrode in the potential range of 1.7−2.7 V became weaker with the increase of exposure time in air. After 12 h of exposure to ambient air, the increased charge capacity of the CS-$LiCoO_2$ was 7 mAh g^{-1} in comparison to the pristine $LiCoO_2$ (Figure 4c), which was about half of the initial increased capacity (15 mAh g^{-1}). Note that 12 h is long enough for the electrode processing and better capacity retention can be achieved in dry rooms that are widely used in battery industry. Correspondingly, the discharge capacity slightly decreased with the increase of exposure time in ambient air. The discharge capacity of the CS-$LiCoO_2$ electrode after 12 h of exposure was close to that of the pristine $LiCoO_2$ (~145 mAh g^{-1}). Good cycling stability was achieved for all of the tested electrodes (Figure 4d), which suggested that the exposure to ambient conditions did not affect the cycling stability of the active $LiCoO_2$ in the CS-$LiCoO_2$. The decrease of the charge capacity is attributed to the side reactions of Li_2O with moisture in the air.

CONCLUSION

In summary, we developed a facile and efficient solution chemistry route to form a built-in prelithiation material on the surface of $LiCoO_2$ to offset the initial lithium loss at the anode and improve the energy density of LIBs. Experimentally, we utilized the chemical reaction between Naph-Li solution and $LiCoO_2$ and enabled the conversion of surficial $LiCoO_2$ into a Li_2O/Co composite nanolayer on $LiCoO_2$ and formed CS-$LiCoO_2$. Typically, a CS-$LiCoO_2$ electrode with 1.5 wt % Li_2O/Co showed 15 mAh g^{-1} higher capacity than the pristine $LiCoO_2$ electrode during the first-cycle charging process. Moreover, a high energy density of 533 Wh kg^{-1} was achieved for the CS-$LiCoO_2$||graphite−SiO cell, which was 52 Wh kg^{-1} higher than the cell using a pristine $LiCoO_2$ electrode. Importantly, such a prelithiation process is facile, cost-effective, and recyclable. It is potentially compatible with the current industrial battery fabrication process as well. We believe that the proposed prelithiation technique will have important applications in the existing as well as next-generation LIB systems utilizing high-capacity Si-based anodes with large first-cycle irreversible lithium loss.

ASSOCIATED CONTENT

Supporting Information

The Supporting Information is available free of charge at https://pubs.acs.org/doi/10.1021/acs.nanolett.0c01413.

https://dx.doi.org/10.1021/acs.nanolett.0c01413
Nano Lett. 2020, 20, 4558−4565

Experimental details; crystal structure of $LiCoO_2$; photographs of the reactants and reaction products; charge/discharge curves of the CS-$LiCoO_2$ electrodes with different degrees of prelithiation; SEM, TEM, and dQ/dV profiles of the pristine $LiCoO_2$ and CS-$LiCoO_2$; XRD, TEM, SEM, and EIS characterizations of the cycled electrodes; and voltage profiles of $LiCoO_2$||graphite/SiO and CS-$LiCoO_2$||graphite/SiO full cells (PDF)

AUTHOR INFORMATION

Corresponding Author

Yongming Sun − *Wuhan National Laboratory for Optoelectronics, Huazhong University of Science and Technology, Wuhan 430074, China;* orcid.org/0000-0001-8528-525X; Email: yongmingsun@hust.edu.cn

Authors

Xiaoxiao Liu − *Wuhan National Laboratory for Optoelectronics, Huazhong University of Science and Technology, Wuhan 430074, China*

Yuchen Tan − *Wuhan National Laboratory for Optoelectronics, Huazhong University of Science and Technology, Wuhan 430074, China*

Wenyu Wang − *Wuhan National Laboratory for Optoelectronics, Huazhong University of Science and Technology, Wuhan 430074, China*

Chunhao Li − *Wuhan National Laboratory for Optoelectronics, Huazhong University of Science and Technology, Wuhan 430074, China*

Zhi Wei Seh − *Institute of Materials Research and Engineering, Agency for Science, Technology and Research (A*STAR), Singapore 138634 Singapore;* orcid.org/0000-0003-0953-567X

Li Wang − *Institute of Nuclear & New Energy Technology, Tsinghua University, Beijing 100084, China*

Complete contact information is available at: https://pubs.acs.org/10.1021/acs.nanolett.0c01413

Notes

The authors declare no competing financial interest.

ACKNOWLEDGMENTS

This work is financially supported by the Natural Science Foundation of China (Grant No. 51802105) and China Postdoctoral Science Foundation (Grant No. 2018M642833). The authors would also like to thank the Analytical and Testing Center of Huazhong University of Science and Technology (HUST) as well as the Center for Nanoscale Characterization & Devices of Wuhan National Laboratory for Optoelectronics (WNLO) for providing the facilities to conduct the characterizations. Z.W.S. acknowledges the support of the Singapore National Research Foundation (NRF-NRFF2017-04).

REFERENCES

(1) Zhang, J.-N.; Li, Q.; Ouyang, C.; Yu, X.; Ge, M.; Huang, X.; Hu, E.; Ma, C.; Li, S.; Xiao, R.; Yang, W.; Chu, Y.; Liu, Y.; Yu, H.; Yang, X.-Q.; Huang, X.; Chen, L.; Li, H. Trace doping of multiple elements enables stable battery cycling of $LiCoO_2$ at 4.6 V. *Nature Energy* **2019**, *4* (7), 594−603.

(2) Liu, T.; Lin, L.; Bi, X.; Tian, L.; Yang, K.; Liu, J.; Li, M.; Chen, Z.; Lu, J.; Amine, K.; Xu, K.; Pan, F. In situ quantification of interphasial chemistry in Li-ion battery. *Nat. Nanotechnol.* **2019**, *14* (1), 50−56.

(3) Scott, I. D.; Jung, Y. S.; Cavanagh, A. S.; Yan, Y.; Dillon, A. C.; George, S. M.; Lee, S. H. Ultrathin coatings on nano-$LiCoO_2$ for Li-ion vehicular applications. *Nano Lett.* **2011**, *11* (2), 414−418.

(4) Qian, J.; Liu, L.; Yang, J.; Li, S.; Wang, X.; Zhuang, H. L.; Lu, Y. Electrochemical surface passivation of $LiCoO_2$ particles at ultrahigh voltage and its applications in lithium-based batteries. *Nat. Commun.* **2018**, *9* (1), 4918.

(5) Tian, T.; Zhang, T. W.; Yin, Y. C.; Tan, Y. H.; Song, Y. H.; Lu, L. L.; Yao, H. B. Blow-Spinning Enabled Precise Doping and Coating for Improving High-Voltage Lithium Cobalt Oxide Cathode Performance. *Nano Lett.* **2020**, *20* (1), 677−685.

(6) Seong, W. M.; Yoon, K.; Lee, M. H.; Jung, S. K.; Kang, K. Unveiling the Intrinsic Cycle Reversibility of a $LiCoO_2$ Electrode at 4.8-V Cutoff Voltage through Subtractive Surface Modification for Lithium-Ion Batteries. *Nano Lett.* **2019**, *19* (1), 29−37.

(7) Duan, H.; Fan, M.; Chen, W.-P.; Li, J.-Y.; Wang, P.-F.; Wang, W.-P.; Shi, J.-L.; Yin, Y.-X.; Wan, L.-J.; Guo, Y.-G. Extended Electrochemical Window of Solid Electrolytes via Heterogeneous Multilayered Structure for High-Voltage Lithium Metal Batteries. *Adv. Mater.* **2019**, *31* (12), No. 1807789.

(8) Zhou, W.; Wang, Z.; Pu, Y.; Li, Y.; Xin, S.; Li, X.; Chen, J.; Goodenough, J. B. Double-Layer Polymer Electrolyte for High-Voltage All-Solid-State Rechargeable Batteries. *Adv. Mater.* **2019**, *31* (4), No. 1805574.

(9) Ren, X.; Zou, L.; Jiao, S.; Mei, D.; Engelhard, M. H.; Li, Q.; Lee, H.; Niu, C.; Adams, B. D.; Wang, C.; Liu, J.; Zhang, J.-G.; Xu, W. High-Concentration Ether Electrolytes for Stable High-Voltage Lithium Metal Batteries. *ACS Energy Lett.* **2019**, *4* (4), 896−902.

(10) Yeom, S. J.; Lee, C.; Kang, S.; Wi, T. U.; Lee, C.; Chae, S.; Cho, J.; Shin, D. O.; Ryu, J.; Lee, H. W. Native Void Space for Maximum Volumetric Capacity in Silicon-Based Anodes. *Nano Lett.* **2019**, *19* (12), 8793−8800.

(11) Liu, T.; Chu, Q.; Yan, C.; Zhang, S.; Lin, Z.; Lu, J. Interweaving 3D Network Binder for High-Areal-Capacity Si Anode through Combined Hard and Soft Polymers. *Adv. Energy Mater.* **2019**, *9* (3), 1802645.

(12) An, W.; Gao, B.; Mei, S.; Xiang, B.; Fu, J.; Wang, L.; Zhang, Q.; Chu, P. K.; Huo, K. Scalable synthesis of ant-nest-like bulk porous silicon for high-performance lithium-ion battery anodes. *Nat. Commun.* **2019**, *10* (1), 1447.

(13) Kim, H. J.; Choi, S.; Lee, S. J.; Seo, M. W.; Lee, J. G.; Deniz, E.; Lee, Y. J.; Kim, E. K.; Choi, J. W. Controlled Prelithiation of Silicon Monoxide for High Performance Lithium-Ion Rechargeable Full Cells. *Nano Lett.* **2016**, *16* (1), 282−288.

(14) Liu, N.; Hu, L.; McDowell, M. T.; Jackson, A.; Cui, Y. Prelithiated silicon nanowires as an anode for lithium ion batteries. *ACS Nano* **2011**, *5* (8), 6487−6493.

(15) Forney, M. W.; Ganter, M. J.; Staub, J. W.; Ridgley, R. D.; Landi, B. J. Prelithiation of Silicon-Carbon Nanotube Anodes for Lithium Ion Batteries by Stabilized Lithium Metal Powder (SLMP). *Nano Lett.* **2013**, *13* (9), 4158−4163.

(16) Zhao, J.; Lu, Z.; Liu, N.; Lee, H. W.; McDowell, M. T.; Cui, Y. Dry-air-stable lithium silicide-lithium oxide core-shell nanoparticles as high-capacity prelithiation reagents. *Nat. Commun.* **2014**, *5*, 5088.

(17) Zhao, J.; Lu, Z.; Wang, H.; Liu, W.; Lee, H.-W.; Yan, K.; Zhuo, D.; Lin, D.; Liu, N.; Cui, Y. Artificial Solid Electrolyte Interphase-Protected Li_xSi Nanoparticles: An Efficient and Stable Prelithiation Reagent for Lithium-Ion Batteries. *J. Am. Chem. Soc.* **2015**, *137* (26), 8372−8375.

(18) Zhao, J.; Sun, J.; Pei, A.; Zhou, G.; Yan, K.; Liu, Y.; Lin, D.; Cui, Y. A general prelithiation approach for group IV elements and corresponding oxides. *Energy Storage Mater.* **2018**, *10*, 275−281.

(19) Park, H.; Yoon, T.; Kim, Y.-U.; Ryu, J. H.; Oh, S. M. Li_2NiO_2 as a sacrificing positive additive for lithium-ion batteries. *Electrochim. Acta* **2013**, *108*, 591−595.

(20) Noh, M.; Cho, J. Role of Li_6CoO_4 Cathode Additive in Li-Ion Cells Containing Low Coulombic Efficiency Anode Material. *J. Electrochem. Soc.* **2012**, *159* (8), A1329−A1334.
(21) Su, X.; Lin, C.; Wang, X.; Maroni, V. A.; Ren, Y.; Johnson, C. S.; Lu, W. A new strategy to mitigate the initial capacity loss of lithium ion batteries. *J. Power Sources* **2016**, *324*, 150−157.
(22) Abouimrane, A.; Cui, Y.; Chen, Z.; Belharouak, I.; Yahia, H. B.; Wu, H.; Assary, R.; Curtiss, L. A.; Amine, K. Enabling high energy density Li-ion batteries through Li_2O activation. *Nano Energy* **2016**, *27*, 196−201.
(23) Bie, Y.; Yang, J.; Wang, J.; Zhou, J.; Nuli, Y. Li_2O_2 as a cathode additive for the initial anode irreversibility compensation in lithium-ion batteries. *Chem. Commun.* **2017**, *53* (59), 8324−8327.
(24) Sun, Y.; Li, Y.; Sun, J.; Li, Y.; Pei, A.; Cui, Y. Stabilized Li_3N for efficient battery cathode prelithiation. *Energy Storage Mater.* **2017**, *6*, 119−124.
(25) Sun, Y. M.; Lee, H. W.; Seh, Z. W.; Liu, N.; Sun, J.; Li, Y. Z.; Cui, Y. High-capacity battery cathode prelithiation to offset initial lithium loss. *Nature Energy* **2016**, *1*, 15008.
(26) Du, J.; Wang, W.; Sheng Eng, A. Y.; Liu, X.; Wan, M.; Seh, Z. W.; Sun, Y. Metal/LiF/Li_2O Nanocomposite for Battery Cathode Prelithiation: Trade-off between Capacity and Stability. *Nano Lett.* **2020**, *20* (1), 546−552.
(27) Sun, Y.; Lee, H.-W.; Zheng, G.; Seh, Z. W.; Sun, J.; Li, Y.; Cui, Y. In Situ Chemical Synthesis of Lithium Fluoride/Metal Nanocomposite for High Capacity Prelithiation of Cathodes. *Nano Lett.* **2016**, *16* (2), 1497−1501.
(28) Liu, Q.; Su, X.; Lei, D.; Qin, Y.; Wen, J.; Guo, F.; Wu, Y. A.; Rong, Y.; Kou, R.; Xiao, X.; Aguesse, F.; Bareno, J.; Ren, Y.; Lu, W.; Li, Y. Approaching the capacity limit of lithium cobalt oxide in lithium ion batteries via lanthanum and aluminium doping. *Nature Energy* **2018**, *3* (11), 936−943.
(29) Nelson Weker, J.; Wise, A. M.; Lim, K.; Shyam, B.; Toney, M. F. Operando Spectroscopic Microscopy of $LiCoO_2$ Cathodes Outside Standard Operating Potentials. *Electrochim. Acta* **2017**, *247*, 977−982.
(30) Shu, J.; Shui, M.; Huang, F.; Ren, Y.; Wang, Q.; Xu, D.; Hou, L. A New Look at Lithium Cobalt Oxide in a Broad Voltage Range for Lithium-Ion Batteries. *J. Phys. Chem. C* **2010**, *114* (7), 3323−3328.
(31) Yang, Z.; Phuong-Vu, O.; He, Y.; Wang, L.; Bowden, M. E.; Xu, W.; Droubay, T. C.; Wang, C.; Sushko, P. V.; Du, Y. Direct Visualization of Li Dendrite Effect on $LiCoO_2$ Cathode by In Situ TEM. *Small* **2018**, *14* (52), No. e1803108.
(32) Liu, X.; Tan, Y.; Liu, T.; Wang, W.; Li, C.; Lu, J.; Sun, Y. A Simple Electrode-Level Chemical Presodiation Route by Solution Spraying to Improve the Energy Density of Sodium-Ion Batteries. *Adv. Funct. Mater.* **2019**, *29* (50), 1903795.
(33) Yuan, X.; Ge, H.; Wang, X.; Dong, C.; Dong, W.; Riaz, M. S.; Xu, Z.; Zhang, J.; Huang, F. Controlled Phase Evolution from Co Nanochains to CoO Nanocubes and Their Application as OER Catalysts. *ACS Energy Lett.* **2017**, *2* (5), 1208−1213.
(34) Huang, X.; Zhang, Y.; Shen, H.; Li, W.; Shen, T.; Ali, Z.; Tang, T.; Guo, S.; Sun, Q.; Hou, Y. N-Doped Carbon Nanosheet Networks with Favorable Active Sites Triggered by Metal Nanoparticles as Bifunctional Oxygen Electrocatalysts. *ACS Energy Lett.* **2018**, *3* (12), 2914−2920.
(35) Cai, Z.; Bi, Y.; Hu, E.; Liu, W.; Dwarica, N.; Tian, Y.; Li, X.; Kuang, Y.; Li, Y.; Yang, X.-Q.; Wang, H.; Sun, X. Single-Crystalline Ultrathin Co_3O_4 Nanosheets with Massive Vacancy Defects for Enhanced Electrocatalysis. *Adv. Energy Mater.* **2018**, *8* (3), 1701694.

https://dx.doi.org/10.1021/acs.nanolett.0c01413
Nano Lett. 2020, 20, 4558−4565